

Isogenic Normal Basal and Luminal Mammary Epithelial Cells Isolated by a Novel Method Show a Differential Response to Ionizing Radiation

Gudrun Huper and Jeffrey R. Marks

Duke University Medical Center, Department of Surgery and Institute for Genome Sciences and Policy, Durham, North Carolina

Abstract

Epithelial cells within the normal breast duct seem to be the primary target for neoplastic transformation events that eventually produce breast cancer. Normal epithelial cells are easily isolated and propagated using standard techniques. However, these techniques almost invariably result in populations of cells that are largely basal in character. Because only ~20% of human breast cancers exhibit a basal phenotype, our understanding of the disease may be skewed by using these cells as the primary comparator to cancer. Further, because germ line mutations in *BRCA1* yield breast cancers that are most often of the basal type, a comparison of normal basal and luminal cells could yield insight into the tissue and cell type specificity of this hereditary cancer susceptibility gene. In this report, we describe a simplified and efficient method for isolating basal and luminal cells from normal human breast tissue. These isogenic cells can be independently propagated and maintain phenotypic markers consistent with their respective lineages. Using these cultured cells, we show that basal and luminal cells exhibit distinct responses to ionizing radiation. Basal cells undergo a rapid but labile cell cycle arrest, whereas luminal cells show a much more durable arrest, primarily at the G₂-M boundary. Molecular markers, including p53 protein accumulation, p53-activated genes, and *BRCA1* nuclear focus formation all correlate with the respective cell cycle responses. Further, we show that short-term cultures of human breast tissue fragments treated with ionizing radiation show a similar phenomenon as indicated by the biphasic accumulation of p53 protein in the basal versus luminal layer. Together, these results indicate that normal basal cells have a transitory cell cycle arrest after DNA damage that may underlie their increased susceptibility to transformation after the loss of functional *BRCA1*. [Cancer Res 2007;67(7):2990–3001]

Introduction

At least two distinct differentiated cell types comprise the normal breast duct. Lining the apical surface of the duct are luminal cells with secretory properties, whereas the basal layer is composed of myoepithelial cells that have properties of both contractile muscle cells and epithelium. Putative stem cell precursors that reside at the growing tip of each duct are believed

to differentiate into these mature cell types. The target cells for breast carcinogenesis have not been fully elucidated. However, it is clear that human breast cancer can be categorized into subtypes that have properties consistent with derivation from both basal and luminal normal mammary epithelia. Basal-type breast cancers are distinguished more through a molecular than a histologic phenotype as they are defined largely by the expression pattern of a series of genes. These cancers typically lack expression of estrogen receptor α (ESR1), progesterone receptor (PGR), and ERBB2 but frequently overexpress epidermal growth factor (EGF) receptor (1). In addition, basal-type breast tumors have a high frequency of TP53 mutations and express a constellation of intermediate filament and extracellular matrix proteins associated with normal basal cells (2, 3). Although other breast cancers lack ESR1, PGR, and ERBB2, and have mutated *TP53*, their expression of structural proteins does not resemble the basal pattern. Luminal types of breast cancers are more heterogeneous and can be subclassified into several categories based on strong signatures related to the combinations of hormone receptors and ERBB2 expression (1).

Contained within the set of basal tumors are the medullary carcinomas (4, 5). Strictly defined, only ~5% of invasive breast cancers fall into this category. However, cancers with several but not all medullary features are more common (atypical medullary carcinoma). Medullary histology is characterized by a circumscribed tumor mass that seems to push at its margins without invading, syncytia formation, and a moderate to heavy number of inflammatory cells, particularly at the periphery of the cancer. These features, particularly the circumscribed growth pattern, may relate to the generally more favorable prognosis of patients with these cancers (6). Aside from their prototypic basal expression profile, this histologic type has also come to prominence due to the abundance of these cancers in *BRCA1* mutation carriers (compared with other histologic subtypes and compared with nonfamilial breast cancers; refs. 7, 8). At the expression level, most *BRCA1* mutation-related cancers are of the basal subtype (9, 10). Further, although somatic mutations in *BRCA1* are extremely uncommon, the *BRCA1* tumor-suppressor gene is hypermethylated in a subset of sporadic breast cancers, notably those with medullary features (11, 12). The weight of evidence indicates that *BRCA1* is involved in the promotion of predominantly basal-type breast cancers.

Normal human breast epithelial cells (HMEC) can be cultured readily, and a number of immortalized lines have been derived. The distinguishing feature of these cells is that they almost uniformly express a strong basal phenotype. Cells with basal properties seem to adhere better to plastic, proliferate more rapidly, and divide more often than cells with luminal characteristics (2, 13). Therefore, basal cells predominate very early during the typical culture of normal mammary epithelial cells from a breast reduction specimen. Within the constraints of tissue culture systems, basal and luminal cells also seem to have different medium/growth

Note: Supplementary data for this article are available at Cancer Research Online (<http://cancerres.aacrjournals.org/>).

Requests for reprints: Jeffrey R. Marks, Department of Surgery, Duke University Medical Center, Durham, NC 27710. Phone: 919-684-6133; E-mail: marks003@mc.duke.edu.

©2007 American Association for Cancer Research.
doi:10.1158/0008-5472.CAN-06-4065

factor requirements (2, 13, 14). Single-cell preparations of primary mammary epithelial cells (derived from ductal fragments or organoids) can be enriched for cells expressing basal [membrane metalloendopeptidase (MME), also called common acute lymphoblastic leukemia antigen (CALLA)] and luminal [MUC1 or epithelial membrane antigen (EMA)] surface antigens using selective antibodies and then propagated to retain their differentiated properties (15). Complex medium formulations have been developed to maintain normal mammary epithelial cells, including fully defined medium (13). Typically, medium containing low serum but supplemented with bovine pituitary extract (BPE) is used to culture HMECs that retain basal characteristics. High serum concentration inhibits the growth of these cells and leads to premature senescence (16). However, cells with luminal properties can be propagated in high serum without BPE. Purified cells grown in this manner can be trans-differentiated by switching to medium containing BPE, but basal cells have not been induced toward luminal growth with this strategy, suggesting that cells in the luminal lineage retain more stem cell characteristics (15).

Germ line mutations in many of the highly penetrant tumor susceptibility genes, including *RB*, *APC*, *BRCA1*, and *BRCA2*, predispose to highly tissue-restricted cancers although their expression and function do not seem to be limited to those specific types of cells. With respect to *BRCA1*, tumor predisposition in the breast seems to be further restricted to cells in the basal lineage. Given the wealth of evidence regarding the function of *BRCA1* in the response to DNA damage, we theorized that basal and luminal cells could have differing responses to damage that might serve to highlight an important facet of *BRCA1*-related tumorigenesis.

Our goal in exploring phenotypic differences in normal breast cells related to *BRCA1* required the reproducible isolation and propagation of both basal and luminal cell types. In this article, we report on a simplified method to separate primary basal and luminal breast epithelial cells and the characterization of cells isolated using this protocol. Further, we have begun to examine these cells after DNA damage and find that isogenic cultures of basal and luminal cells show consistent and unique responses. Basal cells undergo a more transient checkpoint response to ionizing radiation than luminal cells. This may be a defining aspect in their differential susceptibility to *BRCA1*-related cancers.

Materials and Methods

Breast tissue, cell preparation, cell separation, and cell culture.

Women undergoing reduction mammoplasty at Duke University Medical Center were consented for tissue donation under an Institutional Review Board-approved protocol. Breast parenchyma not needed for diagnosis was obtained from surgical pathology and transported to the research laboratory at room temperature the same day as the surgery in DMEM containing 10% fetal bovine serum (FBS).

For preparation of unfractionated normal mammary epithelial cells, organoids were prepared using a protocol adapted from Band and Sager (17) that we had previously modified. One further modification of this protocol was the elimination of filtration and the substitution of two sequential 30 min $1 \times g$ sedimentation steps with fresh medium. After each sedimentation step, the supernatant containing mostly stromal cells was discarded. The remaining pellet contained the epithelial-rich organoids. Organoids were either frozen viably or allowed to settle in tissue culture dishes in DFCI to induce epithelial cell outgrowth.

To obtain single-cell suspensions, either fresh or frozen organoids were washed twice with DMEM containing 1% FBS and once in cold PBS before digestion with trypsin/EDTA (0.05%/0.02% in PBS) for 20 min at 37°C. Digestion was stopped by dilution with cold DMEM + 10% FBS. Cell

preparations were then washed twice with DMEM + 1% FBS and the cell pellet was resuspended in DFCI or BCM (18) medium and filtered through a 100- μ m cell sieve. The single-cell suspension was cultured overnight in either DFCI or BCM containing 5 ng/mL hepatocyte growth factor (HGF). The following day, the cells were trypsinized, washed once in PBS, and counted using a hemocytometer.

For fluorescence-activated cell sorting (FACS), 1×10^7 cells were first blocked in 1 mL of PBS containing 2% normal goat serum + 1% FBS for 15 min on ice with occasional shaking. Cells were then washed once with PBS + 1% FBS, incubated in 1 mL of the monoclonal antibody, Ber-EP4 (DAKO, Carpinteria, CA), at 40 μ g/mL in PBS + 1% FBS for 60 min at 4°C with gentle shaking, followed by three washes with PBS + 1% FBS. In other experiments, cells were sorted based on cell surface staining for CALLA using the J5 antibody (Beckman Coulter, Fullerton, CA) or an antibody to EMA E29 (DAKO), both at 40 μ g/mL. For detection, the cells were then incubated with 1 mL of FITC-conjugated goat anti-mouse IgG (Jackson ImmunoResearch Laboratories, West Grove, PA) at a 1:75 dilution in PBS + 1% FBS at 4°C for 30 min with gentle mixing, washed thrice with PBS + 1% FBS, then finally resuspended in 1 mL DMEM + 10% FBS and 20 units DNase to prevent clumping. The cells were then sorted based on intensity of green fluorescence using a BD FACS Vantage SE instrument and collected in DMEM + 10% FBS. The sorted cells were then centrifuged and plated on 60-mm dishes in the appropriate medium (cells with high Ber-EP4 reactivity in BCM and cells with low reactivity in DFCI).

For growth in three-dimensional culture, Matrigel (BD Biosciences, San Jose, CA) was mixed at a 1:1 ratio with DMEM as a basal medium (no additives). The constituted matrix was solidified at 37°C for 30 min. Cells were then added in the particular full growth medium (either DFCI or BCM) as an overlay to the matrix. For a single well of a 24-well dish, 2.5×10^5 cells were used on 400 μ L of matrix. Fresh medium (DFCI or BCM) was added every other day.

To study the reaction of normal mammary tissue to ionizing radiation, a fresh reduction mammoplasty specimen was trimmed of fat and cut into $\sim 3\text{-mm}^3$ pieces before overnight incubation in DFCI medium in 60-mm tissue culture dishes. The tissue fragments were treated with 5 Gy of ionizing radiation; several pieces were harvested at each time point, frozen in optimum cutting temperature solution, and stored at -80°C for sectioning and immunohistologic analysis.

Gene expression array. Three replicate cultures of Ber-EP4-positive and Ber-EP4-negative cells were cultured in BCM and DFCI, respectively, until $\sim 60\%$ confluent. Total RNA was extracted using the Qiagen Rneasy Mini kit. The quality of the RNA was verified by an Agilent 2100 Bioanalyzer. Labeled probes for Affymetrix DNA microarray analysis were prepared according to the manufacturer's instructions. Biotin-labeled cRNA, produced by *in vitro* transcription, was fragmented and hybridized to the Affymetrix U133A GeneChip arrays (22,283 probe sets,¹ Affymetrix, Santa Clara, CA) at 45°C for 16 h and then washed and stained using the GeneChip Fluidics Station. The arrays were scanned to a target intensity of 500 by a GeneArray Scamer and patterns of hybridization detected as light emitted from the fluorescent reporter groups incorporated into the target and hybridized to oligonucleotide probes. The microarray data (MAS5 format) is available online.²

Irradiation, cell cycle, and side population analysis. Cells and tissue fragments were treated with ionizing radiation using a 137-Cs irradiator. To examine cell cycle after treatment, cells were stained for DNA content with propidium iodide. Briefly, cells were trypsinized and fixed in 2% paraformaldehyde for 30 min at room temperature. After washing with PBS, cells were permeabilized with 70% ethanol (in PBS) at 4°C for 30 min. Cells were then washed in PBS and resuspended in 0.5 mL of PBS containing 100 μ g/mL RNase A and 50 μ g/mL propidium iodide (Invitrogen, Carlsbad, CA) and DNA content was quantitated by flow cytometry using the Duke Comprehensive Cancer Center Shared Flow Cytometry Resource.

To detect, quantitate, and identify the side population of cells that can exclude dye via active pumping, we adapted a protocol described by Dontu

¹ <http://www.affymetrix.com/support/technical/byproduct.affx?product=hgu133>

² <http://data.cgt.duke.edu/Basalluminalradiation.php>

et al. (19). Cryopreserved cultures of very early passage HMEC (not fractionated) were thawed and grown in DFCI overnight before analysis. Cells were then trypsinized and resuspended at a concentration of 1×10^6 /mL in side population medium consisting of Hamm's F12 containing 5 μ g/mL insulin, 1 μ g/mL hydrocortisone, 10 μ g/mL cholera toxin, 10 ng/mL EGF, and 5% FBS. To these suspended cells, we added Hoechst 33342 to 2.5 μ g/mL and verapamil to 50 μ g/mL (and cells were analyzed in parallel with no verapamil) and then incubated for 75 min at 37°C with gentle shaking. After this incubation, the cells were washed twice with ice-cold HBSS. The cells were then resuspended in 0.5 mL HBSS + 2% normal goat serum and 2% FBS and incubated for 15 min on ice. The cells were then centrifuged and resuspended in HBSS + 2% FBS and 40 μ g/mL Ber-EP4 and incubated for 30 min at 4°C with shaking. Cells were then washed twice (HBSS + 2% FBS) before the addition of a FITC-conjugated goat anti-mouse IgG at a 1:75 dilution for 20 min at 4°C. Cells were then washed thrice and resuspended in HBSS + 5% FBS, 2 μ g/mL propidium iodide, and 20 units of DNase to prevent clumping. Cells were then subjected to flow cytometry in a combined analysis for cell surface staining by Ber-EP4 (FITC) to identify basal versus luminal cells and Hoechst dye (UV) to identify the side population through the comparison of cells treated in the presence or absence of verapamil.

Immunoblotting. Whole-cell protein lysates were prepared using a 1% NP40 lysis buffer [150 mmol/L NaCl, 50 mmol/L Tris (pH 8), 1% NP40] supplemented with protease inhibitors. Cells were lysed for 30 min at 4°C, and protein concentrations were quantitated using the Bradford assay. Protein (100 μ g) was separated by SDS-PAGE and then electrotransferred onto nitrocellulose. After blocking in 5% dried milk and PBS-T, antibodies to the following proteins were used for detection: KRT18 (1 μ g/mL AB-2, Calbiochem, San Diego, CA), vimentin (0.5 μ g/mL AB-1, Calbiochem), p53 (0.2 μ g/mL DO1, Calbiochem) and p63 (2 μ g/mL 4A4, Santa Cruz Biotechnology, Santa Cruz, CA), and β -actin (0.1 μ g/mL, Roche Applied Science, Indianapolis, IN). Chemiluminescence (NEN Renaissance) was done after incubating blots in an anti-mouse secondary antibody conjugated to horseradish peroxidase (1:5,000 dilution, Jackson Immuno-Research Laboratories, Inc.).

Northern blotting. Total RNA was extracted from cells using the Qiagen RNeasy Mini kit. Detection of specific mRNAs was carried out after formaldehyde-agarose gel electrophoresis of 10 μ g of total RNA and electrotransfer as previously described (20). Radiolabeled probes were prepared from cloned cDNA inserts of *GADD45A* and *I4-3-3 σ* .

Quantitative real-time PCR. Real-time PCR (RT-PCR) for CDKN1A (p21/CIP1/WAF1) was done using a LightCycler (Roche Applied Science). Primer

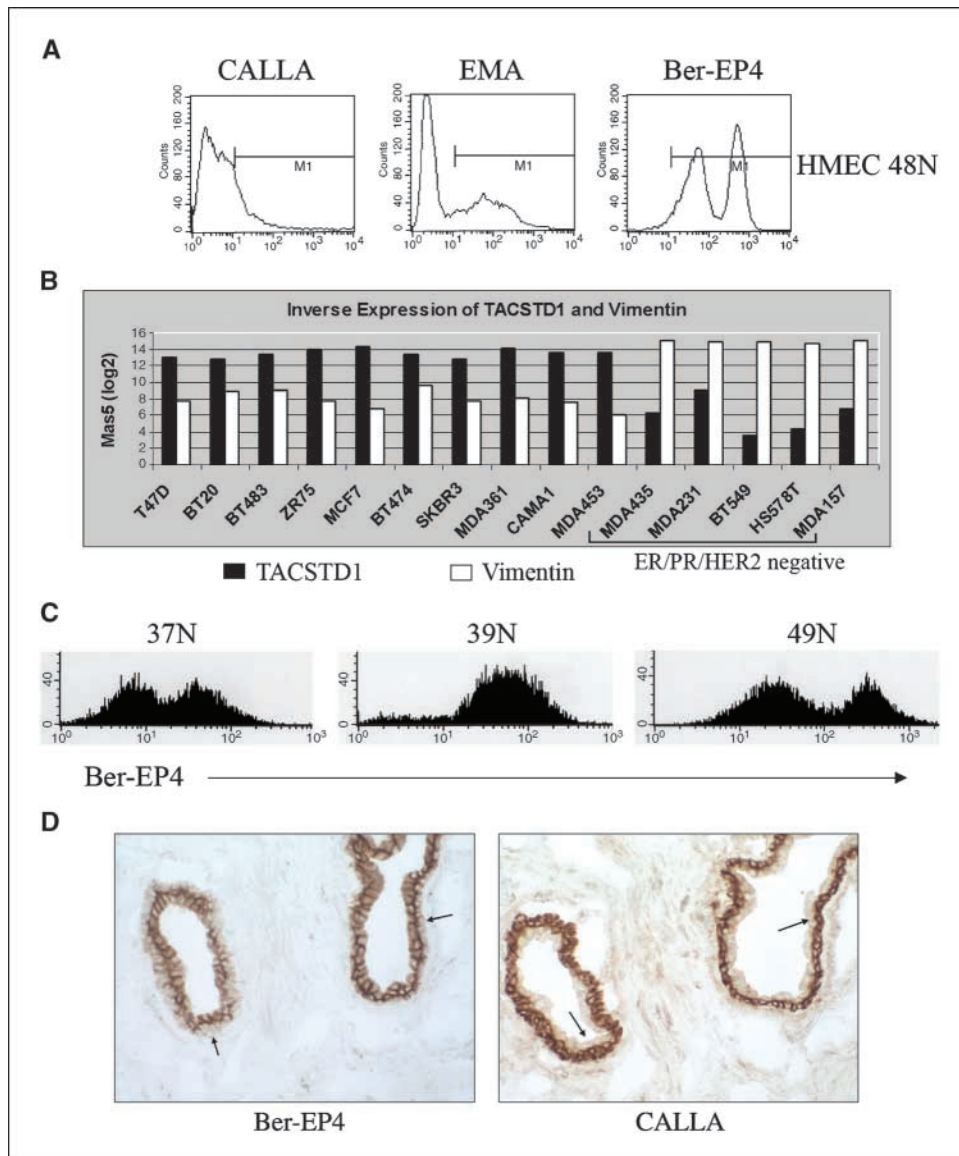


Figure 1. Expression of cell surface antigens on breast epithelial cells. *A*, flow cytometric profile of primary normal mammary epithelial cells with antibodies to CALLA, EMA, and TACSTD1 (Ber-EP4). *B*, expression of *TACSTD1* mRNA in a series of breast cancer cell lines. Columns, MAS5 data log₂-transformed from a single array (Affymetrix Hu133plus) for each cell line. *C*, Ber-EP4 profile of three individual HMEC isolates. The typical profile showing two peaks was observed in 7 of 10 HMEC cultures from different reduction mammoplasties. The remaining three isolates yielded a single primary peak. *D*, normal breast tissue stained with the Ber-EP4 antibody (left) and a parallel section stained with the CALLA antibody (right). Note the inverse staining pattern for basal and luminal cells with these two antibodies, with the Ber-EP4 primarily staining the luminal cells and CALLA reacting with the basal cells.

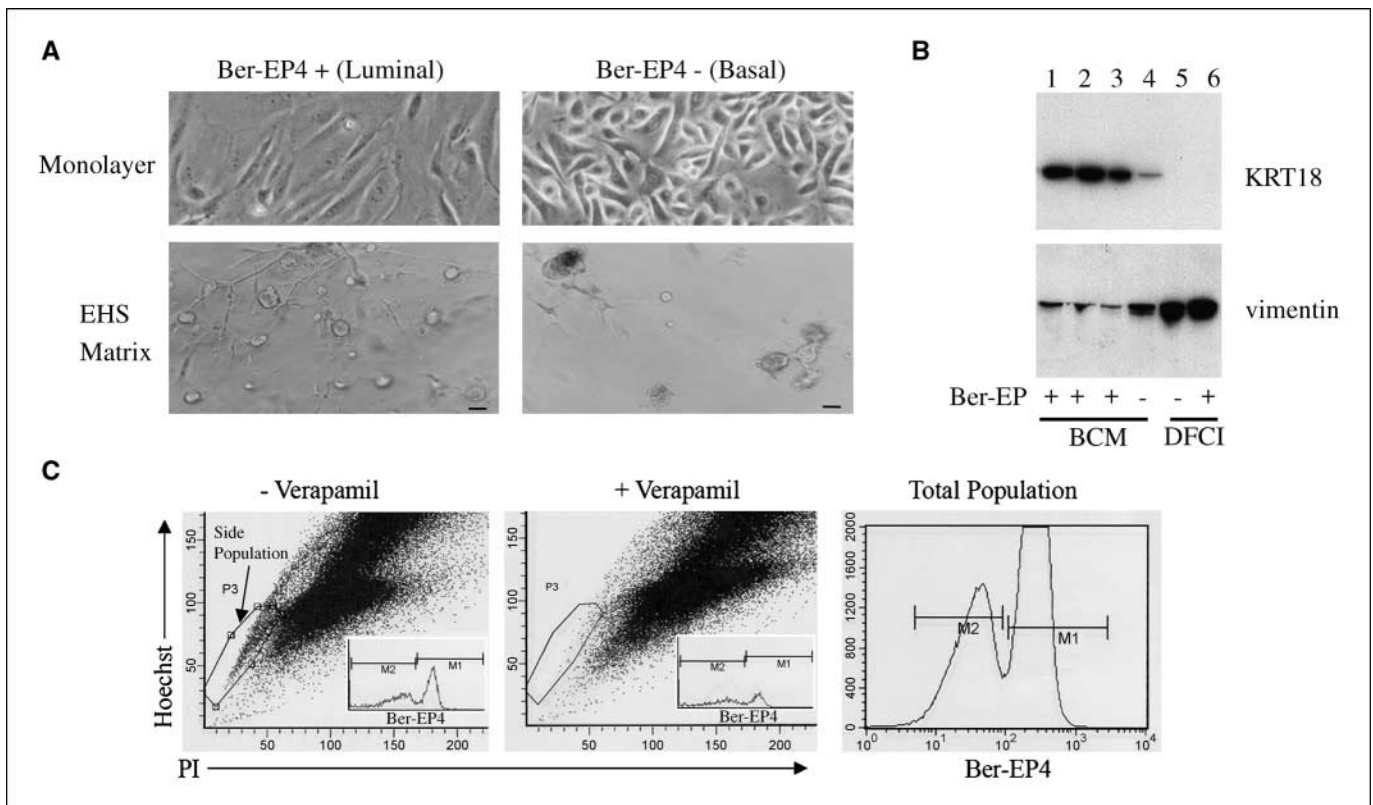


Figure 2. Properties of HMEC sorted by Ber-EP4 reactivity. **A**, HMEC were physically sorted based on cell surface staining with the Ber-EP4 antibody and placed into the appropriate selective medium; that is, cells with high-level reactivity (luminal cells) were placed into BCM and cells with low reactivity (basal cells) were placed into DFCI. Cells were then grown for 8 d in monolayer or three-dimensional cultures (in Matrigel constituted in DFCI) and imaged by phase contrast photomicroscopy. Bar, 50 μ m. **B**, immunoblot of protein extracted from monolayer cultures of HMEC sorted by Ber-EP4 staining. *Top blot*, probed for KRT18; *bottom blot*, from the same protein extracts, probed with an antibody to vimentin. *Lanes 1 to 3*, Ber-EP4 positive cells (luminal) cultured in BCM; *lane 4*, Ber-EP4 negative (basal) cultured in BCM; *lane 5*, Ber-EP4 negative (basal) cultured in DFCI; *lane 6*, Ber-EP4 positive (luminal) cultured in DFCI. HGF (*lane 1*, 5 ng/mL) and prolactin (*lane 2*, 5 μ g/mL) were added to the BCM. KRT18 migrated at 45 kDa and vimentin at 58 kDa. For subsequent experiments with luminal cells and BCM, HGF was added to all plates. **C**, analysis of side population in HMEC. Unfractionated primary HMEC were incubated with Hoechst 33342 for 75 min in the presence or absence of 50 μ g/mL verapamil. The cells were then stained with the Ber-EP4 antibody and a secondary antibody conjugated with FITC. The cells were then incubated with propidium iodide (PI) and analyzed by flow cytometry. Gating of the side population was guided by the difference between verapamil-treated and untreated cells, and this population was then analyzed for Ber-EP4 intensity. Both Ber-EP4-positive and Ber-EP4-negative cells were equally diminished after verapamil treatment, indicating that the side population was evenly distributed between basal and luminal cells.

sequences for *CDKN1A* were as follows: forward-TCAGGGGAGCAGGC-TGAA and reverse-TTTGAGGCCTCGCCTT, yielding a 175-bp product spanning the second and third exons. In parallel reactions, glyceraldehyde-3-phosphate dehydrogenase (*GAPDH*) cDNA was quantitated for normalization. The reaction mixtures contained 2 μ L Titanium PCR buffer (Clontech, Mountain View, CA), 1 μ L 100 \times bovine serum albumin (BSA; New England Biolabs, Ipswich, MA), 1 \times SYBR Green I (Invitrogen), 0.5 mmol/L deoxynucleotide triphosphates, 0.25 μ mol/L of forward and reverse primers, 1 \times AdvanTaqPlus polymerase (Clontech), and 50 ng cDNA. The cycling profile included a hot start at 95 $^{\circ}$ C for 120 s followed by 40 cycles of a denaturation step at 95 $^{\circ}$ C for 0 s, 58 $^{\circ}$ C annealing for 10 s, 72 $^{\circ}$ C of extension for 12 s, and a fluorescent signal acquisition at 84 $^{\circ}$ C.

Immunohistochemistry and immunofluorescence. To detect p53, CALLA, and phosphorylated H2AX in *ex vivo* cultured breast tissue, 5- μ m frozen sections were cut and air dried. Before staining, sections were fixed in acetone at room temperature, dried for 15 min, and then blocked with 5% horse serum for 15 min. The primary antibody was then applied for 1 h at room temperature. Monoclonal antibodies to the following antigens were used: p53 (0.2 μ g/mL DO1, Calbiochem), CALLA (10 μ g/mL J5 for CALLA, Coulter), and p-H2AX (10 μ g/mL, Upstate, Lake Placid, NY). Slides were then washed thrice in PBS at which time the sections were incubated with the biotinylated secondary antibody (1:100 horse anti-mouse, Vector Laboratories, Burlingame, CA) for 30 min at room temperature. Sections

were again washed thrice in PBS and then incubated with the avidin/biotinylated enzyme complex (Vector Laboratories) for 30 min at room temperature. The slides were washed thrice in PBS and then incubated with 0.05% 3,3'-diaminobenzidine for 3.5 min at room temperature. The slides were then washed extensively in running tap water before counterstaining with methyl green. Coverslips were mounted after dehydration in graded ethanol and clearing in xylene.

For immunofluorescent detection of the BRCA1 protein, 2×10^4 cells were deposited onto microscope slides using a Shandon cytocentrifuge and then air dried for 2 h at room temperature. Cells were fixed in 100% methanol at -20 $^{\circ}$ C for 10 min, air dried for 5 min, then further permeabilized with 0.1% Triton X-100 in PBS for 5 min at room temperature. Before antibody detection, cells were blocked for 1 h at room temperature in PBS containing 5% goat serum, 1% glycerol, 0.1% BSA, and 0.1% fish skin gelatin (blocking buffer). Cells were then incubated with the primary monoclonal antibody [anti-BRCA1, 1 μ g/mL of MS110 (Calbiochem) or mouse IgG1] at 4 $^{\circ}$ C overnight in blocking buffer. The next day, slides were washed thrice in PBS before the secondary antibody was applied (1:500 goat anti-mouse conjugated with AlexaFluor 488, Molecular Probes) in blocking buffer for 1 h at room temperature. The slides were then washed thrice in PBS, postfixed in 4% paraformaldehyde for 5 min, washed twice in PBS, and then stained for 5 min with 1 μ g/mL Hoechst 33342 in PBS. Slides were then washed twice in water, air-dried, and coverslips were mounted with Vectashield (Vector Laboratories).

Table 1. Genes most differentially expressed in basal versus luminal cells

| Basal | | | | | Luminal | | | | |
|-------------|-----------------|-------|---------|-----|-------------|-----------------|-------|---------|------|
| Probe ID | Gene | Jones | Allinen | S | Probe ID | Gene | Jones | Allinen | S |
| 205064_at | <i>SPRR1B</i> | + | | 8.1 | 210095_s_at | <i>IGFBP3</i> | | | -6.1 |
| 205916_at | <i>S100A7</i> | + | | 7.3 | 201596_x_at | <i>KRT18</i> | | | -6.0 |
| 203691_at | <i>PI3</i> | | | 7.2 | 209008_x_at | <i>KRT8</i> | | + | -5.2 |
| 202917_s_at | <i>S100A8</i> | | | 5.5 | 201650_at | <i>KRT19</i> | | + | -3.8 |
| 203535_at | <i>S100A9</i> | | | 5.1 | 213711_at | <i>KRTHB1</i> | | | -3.6 |
| 209800_at | <i>KRT16</i> | | | 4.9 | 210046_s_at | <i>IDH2</i> | | | -2.9 |
| 214599_at | <i>IVL</i> | | | 4.6 | 209140_x_at | <i>HLA-B</i> | | | -2.8 |
| 214549_x_at | <i>SPRR1A</i> | | | 3.8 | 206595_at | <i>CST6</i> | + | | -2.6 |
| 214580_x_at | <i>KRT6B</i> | | | 3.8 | 210764_s_at | <i>CYR61</i> | | | -2.2 |
| 207065_at | <i>K6HF</i> | | | 3.6 | 209040_s_at | <i>PSMB8</i> | | | -2.2 |
| 200632_s_at | <i>NDRG1</i> | | | 3.5 | 208729_x_at | <i>HLA-B</i> | | | -2.1 |
| 214164_x_at | <i>AP1G1</i> | | | 3.4 | 204279_at | <i>PSMB9</i> | | | -2.0 |
| 218717_s_at | <i>LEPREL1</i> | | | 3.3 | 212143_s_at | <i>IGFBP3</i> | | | -2.0 |
| 39248_at | <i>AQP3</i> | | | 3.1 | 206074_s_at | <i>HMGIIY</i> | | | -1.9 |
| 219250_s_at | <i>FLRT3</i> | | | 2.9 | 211911_x_at | <i>HLA-B</i> | | | -1.7 |
| 204971_at | <i>CSTA</i> | + | | 2.8 | 206670_s_at | <i>GAD1</i> | | | -1.6 |
| 219554_at | <i>RHCG</i> | | | 2.7 | 209121_x_at | <i>NR2F2</i> | | | -1.6 |
| 204455_at | <i>BPAG1</i> | + | + | 2.7 | 204733_at | <i>KLK6</i> | + | | -1.6 |
| 215177_s_at | <i>ITGA6</i> | + | | 2.6 | 204734_at | <i>KRT15</i> | | | -1.5 |
| 203963_at | <i>CA12</i> | | | 2.6 | 203828_s_at | <i>NK4</i> | + | | -1.5 |
| 209699_x_at | <i>AKRIC2</i> | + | | 2.5 | 218966_at | <i>MYO5C</i> | | | -1.4 |
| 210735_s_at | <i>CA12</i> | | | 2.4 | 208812_x_at | <i>HLA-C</i> | | | -1.4 |
| 209863_s_at | <i>TP73L</i> | + | + | 2.3 | 202510_s_at | <i>TNFAIP2</i> | + | | -1.4 |
| 204855_at | <i>SERPINB5</i> | + | | 2.3 | 201508_at | <i>IGFBP4</i> | | | -1.3 |
| 203562_at | <i>FEZ1</i> | | | 2.3 | 202888_s_at | <i>ANPEP</i> | | | -1.3 |
| 206033_s_at | <i>DSC3</i> | | | 2.2 | 212444_at | <i>FLJ22182</i> | | | -1.3 |
| 205067_at | <i>IL1B</i> | | | 2.2 | 206669_at | <i>GAD1</i> | | | -1.3 |
| 202088_at | <i>SLC39A6</i> | | | 2.2 | 203108_at | <i>RAI3</i> | | | -1.3 |
| 206156_at | <i>GJB5</i> | | | 2.2 | 201445_at | <i>CNN3</i> | | | -1.2 |
| 202504_at | <i>TRIM29</i> | + | | 2.1 | 209094_at | <i>DDAH1</i> | | | -1.2 |
| 222108_at | <i>AMIGO2</i> | | | 2.1 | 212481_s_at | <i>TPM4</i> | | | -1.2 |
| 216268_s_at | <i>JAG1</i> | + | | 2.0 | 205258_at | <i>INHBB</i> | | | -1.2 |
| 210118_s_at | <i>IL1A</i> | | | 1.9 | 219051_x_at | <i>METRNL</i> | | | -1.1 |
| 206032_at | <i>DSC3</i> | | | 1.9 | 219935_at | <i>ADAMTS5</i> | | | -1.0 |
| 209758_s_at | <i>MFAP5</i> | | | 1.9 | 211799_x_at | <i>HLA-C</i> | | | -1.0 |
| 210355_at | <i>PTH1LH</i> | + | | 1.9 | 201952_at | <i>ALCAM</i> | | | -1.0 |
| 201667_at | <i>GJA1</i> | | | 1.9 | 205780_at | <i>BIK</i> | | | -1.0 |
| 211756_at | <i>PTH1LH</i> | + | | 1.9 | 202838_at | <i>FUCA1</i> | | | -1.0 |
| 209569_x_at | <i>D4S234E</i> | | | 1.8 | 217867_x_at | <i>BACE2</i> | + | | -1.0 |
| 204351_at | <i>S100P</i> | | | 1.8 | 203215_s_at | <i>MYO6</i> | | | -1.0 |
| 203021_at | <i>SLPI</i> | | | 1.8 | 203892_at | <i>WFDC2</i> | + | | -1.0 |
| 202831_at | <i>GPX2</i> | | | 1.7 | 209581_at | <i>HRASLS3</i> | | | -1.0 |
| 204469_at | <i>PTPRZ1</i> | | | 1.7 | 204881_s_at | <i>UGCG</i> | | | -1.0 |
| 221854_at | <i>PKP1</i> | | | 1.7 | 201842_s_at | <i>EFEMP1</i> | | | -0.9 |
| 204151_x_at | <i>AKRIC1</i> | | | 1.7 | 201313_at | <i>ENO2</i> | | | -0.9 |
| 209125_at | <i>KRT6A</i> | | | 1.6 | 218211_s_at | <i>MLPH</i> | | | -0.9 |
| 201185_at | <i>PRSS11</i> | + | | 1.6 | 212531_at | <i>LCN2</i> | + | | -0.9 |
| 210809_s_at | <i>POSTN</i> | | | 1.6 | 209373_at | <i>BENE</i> | | | -0.8 |
| 214370_at | <i>S100A8</i> | | | 1.5 | 201428_at | <i>CLDN4</i> | + | + | -0.8 |
| 213765_at | <i>MFAP5</i> | | | 1.5 | 203071_at | <i>SEMA3B</i> | + | | -0.8 |
| 206165_s_at | <i>CLCA2</i> | | | 1.5 | 206200_s_at | <i>ANXA11</i> | | | -0.8 |
| 206400_at | <i>LGALS7</i> | + | | 1.5 | 214088_s_at | <i>FUT3</i> | | | -0.8 |
| 204879_at | <i>TIA-2</i> | | | 1.5 | 205044_at | <i>GABRP</i> | | | -0.7 |
| 206642_at | <i>DSG1</i> | | | 1.5 | 204304_s_at | <i>PROM1</i> | | | -0.7 |
| 202089_s_at | <i>SLC39A6</i> | | | 1.5 | 201825_s_at | <i>SCCPDH</i> | | | -0.7 |
| 211194_s_at | <i>TP73L</i> | + | + | 1.4 | 206560_s_at | <i>MIA</i> | | | -0.7 |

(Continued on the following page)

Table 1. Genes most differentially expressed in basal versus luminal cells (Cont'd)

| Basal | | | | | Luminal | | | | |
|-------------|-----------------|-------|---------|-----|-------------|---------------|-------|---------|------|
| Probe ID | Gene | Jones | Allinen | S | Probe ID | Gene | Jones | Allinen | S |
| 218002_s_at | <i>SCYB14</i> | | | 1.4 | 204602_at | <i>DKK1</i> | | | -0.7 |
| 201287_s_at | <i>SDC1</i> | | | 1.4 | 209120_at | <i>NR2F2</i> | | | -0.7 |
| 209099_x_at | <i>JAG1</i> | + | | 1.4 | 203570_at | <i>LOXL1</i> | | | -0.7 |
| 202345_s_at | <i>FABP5</i> | + | | 1.4 | 204806_x_at | <i>HLA-F</i> | | | -0.7 |
| 206300_s_at | <i>PTHLH</i> | + | | 1.4 | 202790_at | <i>CLDN7</i> | | | -0.7 |
| 212190_at | <i>SERPINE2</i> | | | 1.3 | 218731_s_at | <i>WARP</i> | | | -0.6 |
| 204268_at | <i>S100A2</i> | + | | 1.3 | 213400_s_at | <i>TBL1</i> | | | -0.6 |
| 205680_at | <i>MMP10</i> | | | 1.3 | 215034_s_at | <i>TM4SF1</i> | | | -0.6 |
| 209260_at | <i>SFN</i> | + | | 1.3 | 215189_at | <i>KRTHB6</i> | | | -0.6 |
| 210367_s_at | <i>PTGES</i> | | | 1.3 | 211529_x_at | <i>HLA-G</i> | | | -0.6 |

NOTE: Genes most differentially expressed were derived by PAM from Hu133 Affymetrix arrays done in triplicate. Genes/probes are listed in decreasing order of association with the PAM scores (*S*). Genes that also show up on the highest ranking differentially expressed genes from Jones et al. (33) and Allinen et al. (34) are indicated.

Results

Separation of basal and luminal mammary epithelial cells.

To study the different cell lineages, we sought to isolate and propagate luminal and basal cells independently from a single preparation of normal human breast tissue. To this end, we attempted to use protocols developed by Pechoux et al. (15) for this purpose. We had extensive experience (21) in preparing organoids and culturing HMEC using techniques pioneered by Band and Sager (17). From breast reduction specimens, primary epithelial cells are typically grown from organoids on plastic. These organoids consist of fragments of ducts and lobules partially digested and purified away from fat and connective tissue. Epithelial cells grow out of the viable organoids and through differential trypsinization and the use of a selective medium contaminating fibroblasts are largely eliminated. Relatively short-term culture produces a morphologically mixed population of adherent cells that can grow rapidly for 2 to 3 weeks with increasing senescence toward the end of this period. Because it is the basal cells that tend to proliferate, immortalization of HMEC invariably results in cell lines that have the basal phenotype. However, by digesting organoids to single cells before culturing, antibody-based separation methods can be used to isolate enriched luminal and basal cell fractions.

Antibodies to CALLA and MUC1 have been used to separate basal and luminal cells (15, 18). In our hands, this approach was inefficient, yielding very few cells from a typical organoid preparation. In examining the profile of cells detected by these antibodies via flow cytometry, we observed very little CALLA reactivity. In contrast, EMA staining intensity showed a bimodal distribution with a peak of cells that are low/negative and a peak with reactivity spanning ~2 orders of magnitude in fluorescent intensity (Fig. 1A). While investigating methods for detecting circulating epithelial cells, we used what was considered to be a pan-epithelial antibody (Ber-EP4) for immunomagnetic enrichment (22). In testing this antibody on a series of breast cancer cell lines, we noted a broad range of reactivity. Lines with basal characteristics stained with less intensity than those considered to be of the luminal type. Gene expression array data on a set of breast cancer cell lines (23) confirmed this finding (Fig. 1B).

The Ber-EP4 antibody detects a 35 to 40 kDa cell surface glycoprotein identified as tumor-associated calcium signal transducer 1 (*TACSTD1*) but also known as epithelial cell adhesion molecule (EpCAM; ref. 24). Reacting early passage normal mammary epithelial cells with Ber-EP4 yielded a clear bimodal distribution with almost all cells falling into two discrete peaks (Fig. 1A). In further testing of this antibody on HMEC from other individuals, we found that this was a typical but not invariant pattern (Fig. 1C). We have analyzed very early passage HMEC from 10 separate reductions in this manner with three yielding only a single peak after Ber-EP4 staining. The other seven showed two discrete peaks containing virtually all of the viable cells.

We suspected that the Ber-EP4 antibody was preferentially staining cells of the luminal lineage and sought to test this possibility. Organoids were digested with trypsin, followed by filtration through 100- μ m mesh to obtain single cells. These cells were incubated with the primary antibody (Ber-EP4) followed by a FITC-conjugated secondary antibody and then subjected to preparative flow sorting. As many as several million cells were reacted and sorted in this manner using a high-speed flow cytometer, and the two peaks were collected separately. Previous studies using other antibody-based separation techniques have shown that distinct culture conditions are required to maintain and grow basal and luminal breast epithelial cells (15, 18). Medium containing BPE and low serum (35 μ g of protein/mL BPE and 1% FCS) supports the growth and maintains the characteristics of basal cells, whereas medium containing high serum (10%) and no pituitary extract promotes the growth of luminal cells. Switching basal cells into high serum leads to arrest and senescence, whereas switching luminal cells into medium containing BPE and reducing the serum leads to trans-differentiation into cells with basal characteristics (15). Cells sorted into high and low Ber-EP4-reactive populations exhibited properties consistent with those previously reported for luminal and basal cells, respectively. Ber-EP4+ cells grown in serum-containing medium (BCM; ref. 18) were more elongated and phase dark than basal cells grown in BPE-containing medium (DFCI; ref. 25; Fig. 2A). Further, the luminal cells grew more quickly into acinar structures in three-dimensional

culture compared with the basal-type cells from the same organoid preparation. Both types of cells eventually grew into large structures (>50 μm in diameter) in DFCI-constituted Matrigel; however, the luminal cells had higher levels of branching extensions (Fig. 2A). Matrigel constituted with BCM (high serum) also supported the growth of both cell types with the luminal cells again showing many more branched structures than isogenic basal cells (not shown). Expression of a series of basal and luminal markers was also examined by immunoblotting. Basal cells showed high levels of vimentin and low levels of cytokeratin 18 (KRT18) when grown in DFCI, whereas luminal cells had the opposite expression pattern when grown in BCM (Fig. 2B). Switching the luminal cells to DFCI resulted in morphologic conversion (not shown) accompanied by a loss of KRT18 and increase in vimentin expression (Fig. 2B, lane 6). All of these properties are consistent with an efficient separation of basal and luminal cells using this single antibody coupled with flow cytometry.

The ready interconversion of luminal to basal cells accomplished by lowering serum and adding pituitary extract suggested a simple set of experiments to discover the substances responsible for this action. We reasoned that pituitary-derived hormones might be able to replace whole pituitary extract in inducing this phenomenon. Therefore, we attempted to recapitulate trans-differentiation by culturing luminal cells in DFCI (low serum) without BPE but in the presence of individual purified pituitary hormones (thyroid stimulating hormone, luteinizing hormone, follicle-stimulating hormone, prolactin, growth hormone, adrenocorticotropic hormone, melanocyte-stimulating hormone, antidiuretic hormone, and oxyto-

cin) and mixtures thereof. We assessed trans-differentiation by morphology and gene expression (vimentin, p63, and KRT19). Unlike the full medium switch, we were unable to induce trans-differentiation using the purified hormones (data not shown). These studies were not exhaustive (one concentration of each hormone was chosen); however, the absence of any evidence of differentiation suggests that it is not under simple one hormone control. The other possibility is that high serum maintains the luminal phenotype and its removal promotes basal differentiation. This is unlikely because low serum was used in conjunction with all of the purified pituitary hormones. We continue to investigate this intriguing system.

Expression array analysis. Cells cultured in their respective medium were subjected to expression analysis using Affymetrix U133A chips (~22,000 probe sets). From this experiment, done in triplicate (separate dishes from the same preparation), the top 50 genes differentially expressed in basal versus luminal cells are listed in Table 1 [determined by prediction analysis of microarrays (PAM); ref. 26]. Many of these genes track with the known cytokeratin profiles of the two cell types. The basal cells have high levels of *KRT2*, *KRT6*, *KRT16*, and *KRT17*, whereas luminal cells express *KRT8*, *KRT18*, and *KRT19* (full data can be found in Supplementary Data). Other known basal markers that show up on this shortened list include *TP73L* (p63), *SERPINB5* (maspin), and members of the S100 family (27, 28). In addition to the distinctive cytokeratin profile, luminal cells express a variety of secreted proteins characteristic of ductal epithelia, including insulin-like growth factor binding proteins (*IGFBP*) 3 and 4, *KLK6*, *WFDC2*, and inhibin (29–32). *TACSTD1* (the antigen recognized by the discriminating

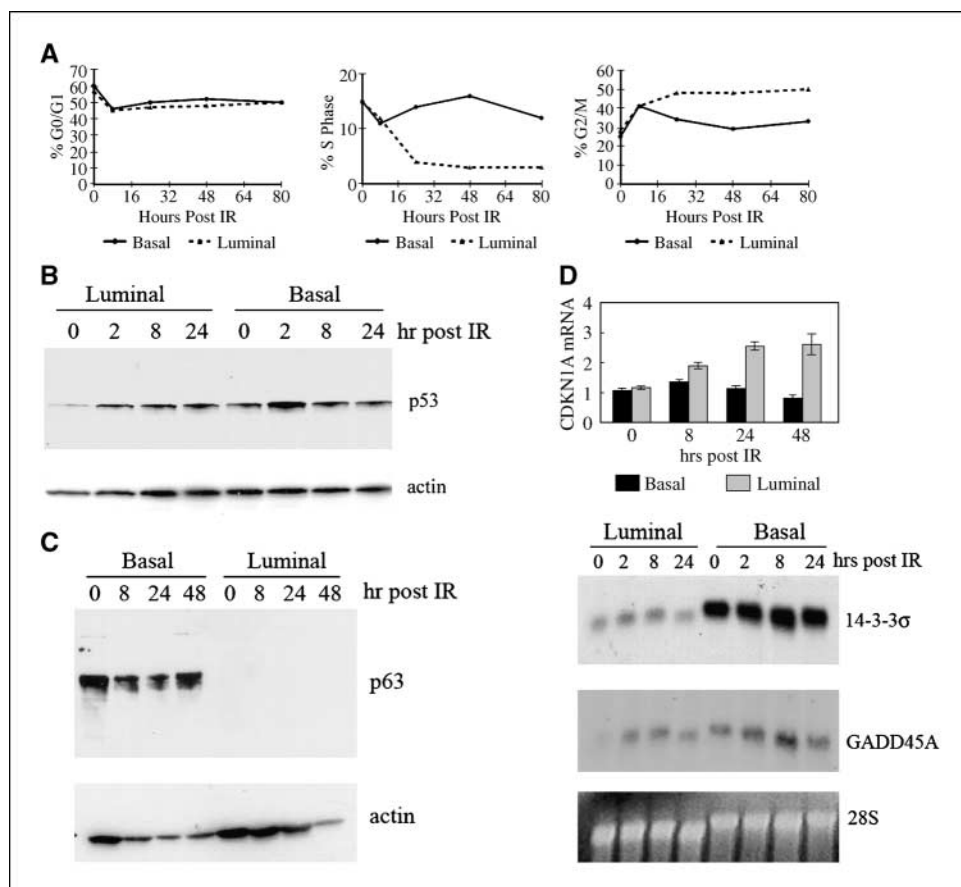


Figure 3. Response of basal and luminal breast epithelial cells to ionizing radiation. *A*, monolayer cultures of basal cells grown in DFCI and luminal cells grown in BCM were treated with 5 Gy of ionizing radiation (*IR*) and then analyzed for cell cycle by propidium iodide staining followed by flow cytometry. At time 0 (before ionizing radiation), both basal and luminal cells displayed equivalent cell cycle fractions. *B*, detection of p53 protein by immunoblotting after ionizing radiation. *C*, detection of p63 protein after ionizing radiation. *D*, detection of mRNA from p53-responsive genes after ionizing radiation. The p21 mRNA was detected by quantitative RT-PCR normalized to GAPDH, whereas 14-3-3 σ and GADD45A were detected by Northern blotting from total RNA.

antibody, Ber-EP4) is 91st on the list of luminal-specific genes with a score of -0.4 .

Because it can be argued that many of the phenotypic properties of these cells may be secondary to the different culture conditions, other groups have purified and examined basal and luminal cell expression patterns without prior culturing. Given the different types of purification and expression analyses that were done, direct comparisons between these studies could be problematic. Nonetheless, we felt it important to compare these data to determine whether our purification and culture conditions retained similar basal and luminal expression patterns. Ranked gene lists from Jones et al. (33) using custom-spotted arrays with $\sim 6,000$ genes reported the top 50 probes from purified basal (38 different genes due to duplicate probes) and luminal cells (37 different genes). From their list of basal cell genes, we could find 36 on the U133A arrays with 30 (83%), demonstrating at least 2-fold greater expression in the appropriate direction. A similar relationship was observed with the set of luminal genes from this study with 29 found on the U133A array and 22 (76%) expressed significantly in the same direction. Allinen et al. (34) used serial analysis of gene expression (SAGE) to study gene expression from purified basal and luminal breast epithelial cells. Of the genes most differentially expressed between the two cell types, SAGE tags representing 18 different genes are provided for basal cells and 25 for luminal cells. We could identify 15 of 18 on the U133A array for the basal cell signature and of these, 6 (40%) were significantly overexpressed in the correct direction. For the luminal cells, 18 of 25 probes are found on the U133A arrays with 8 (44%) showing a similar pattern of expression. None of the genes in these comparisons trended in the opposite direction. Overall, this seems to be extremely good concordance given the issues of purification, culture conditions, and expression analysis platforms. The lower concordance with the SAGE results is not surprising, and we note that many of the genes that do not correlate have very low expression levels (scored as absent) on the Affymetrix arrays, suggesting that the two methods may be somewhat complementary in their sensitivity for different genes. This comparison does reinforce that each of the purification strategies results in similar types of cells, and each group has consistently identified and named the two cell types. Further, it indicates that our short-term culture conditions maintain the appropriate differentiated status.

Side population is evenly distributed between basal and luminal cells. It has been suggested that luminal cells may contain the putative breast stem cell because they can be induced to convert to the basal phenotype (15). A shared characteristic of many stem cells is their ability to pump out and thus exclude dyes such as Hoechst 33342 by virtue of the expression of various transporter proteins (35). The activity of these transporters can be blocked by the calcium ion flux inhibitor, verapamil. By incubating cells with a dye followed by flow cytometric analysis, a so-called side population can be identified by comparing cells treated in the presence or absence of verapamil. The side population consists of cells that are able to pump out the dye and thus appear distinct from the majority of cells that take up dye. We did such an experiment on a series of unfractionated normal mammary epithelial cells. By also staining the treated cells with Ber-EP4, we were able to determine which fraction (basal or luminal) was enriched for side population cells (Fig. 2C). In all cases, the side population was evenly distributed between cells with high and low Ber-EP4 staining, implying that this putative stem cell characteristic does not track closely with either

population. Although we obtained different levels of basal and luminal cells from each HMEC preparation (see Fig. 1C), verapamil treatment in each case reduced the two fractions equally.

Differential response to ionizing radiation. We initially hypothesized that the different lineages might respond distinctly to DNA damage accounting for the phenotypic properties of BRCA1-related breast cancers. To test this, matched luminal and basal cultures were subjected to 5 Gy of ionizing radiation, harvested at varying time points, and analyzed for cell cycle distribution by flow cytometry (a representative experiment is shown in Fig. 3A). Results from these experiments showed that luminal cells enter into a prolonged cell cycle arrest, primarily accumulating in G₂-M. Basal cells undergo arrest, also largely in G₂-M, but resume cycling within 24 h after irradiation. The latest time point for any of our experiments was 80 h and within this time frame, neither cell type showed an increase in subdiploid or hypertetraploid populations. Viability as measured by trypan blue exclusion and side scatter was not reduced over the course of the experiment in either cell type.

Induction of p53 protein tends to be a critical and early event in response to DNA damage, particularly in normal primary cells. We examined time points over the course of 24 h after 5 Gy of ionizing radiation for p53 protein accumulation (Fig. 3B). Luminal cells had lower baseline levels of p53 protein compared with matched basal cells. Both cell types induced p53 protein by 2 h, but basal cells returned to baseline levels by 8 h, whereas p53 protein remained elevated in the luminal cell type. A p53 homologue that also has transactivation properties, p63 (TP73L), was also examined at the protein level. As previously reported, this is an excellent myoepithelial cell marker that is expressed in the breast almost exclusively in the basal layer (27, 36). The fractionated cells completely mirror this pattern with high-level expression in the basal cells and no detectable expression in the matched luminal cultures (Fig. 3C). However, ionizing radiation did not induce p63 protein levels in either cell type.

Consequences of p53 stabilization after DNA damage include transcriptional activation of a number of genes that can lead to cell cycle arrest, either at the G₁-S or G₂-M boundaries. We examined mRNA levels of several of the most prominent candidates in these cells (Fig. 3D). *CDKN1A* (*p21*) is strongly induced in wild-type p53 breast epithelial cells after DNA damage. For example, irradiation of the MCF7 breast cancer cell line produces a robust p53 and *p21* response concomitant with a prolonged G₁ arrest (37).³ The magnitude and duration of the *p21* response in our sorted populations was measured by quantitative RT-PCR normalized to *GAPDH* expression. As we have observed before with unselected normal mammary epithelial cells grown in DFCI (i.e., cells that are predominantly basal), *p21* is not highly induced and returns to baseline levels quickly. In other experiments (data not shown), maximal induction in basal cells occurs 4 h after ionizing radiation. This is consistent with the brief accumulation of p53 in these cells. In contrast, purified luminal cells displayed a prolonged increase in *p21* mRNA levels matching the durable increase in steady-state p53 protein. Other p53-responsive genes more tightly associated with G₂-M arrest were also examined by Northern blotting. Luminal cells showed a prolonged increase in *GADD45A* (similar to *p21*), whereas *Stratifin* (*SFN*, *14-3-3 σ*) was not induced in either population. Previous studies have shown that *SFN* is highly expressed in

³ J.R. Marks, unpublished data.

normal mammary epithelial cells and silenced by hypermethylation in a high percentage of invasive breast cancers (38). Our current data indicate that *SFN* expression is heavily skewed toward basal cells, and loss of expression in most breast cancers may be associated not only with hypermethylation but also with the lineage of the cancer (i.e., basal versus luminal).

Starting from first principles, we anticipated that BRCA1 could play a distinct role in response to DNA damage in the two cell populations. One measure of BRCA1 action is the accumulation of the BRCA1 protein into nuclear foci (39). These foci accumulate at sites of DNA damage with a variety of other members of the repair machinery (40). Matched luminal and basal cells were treated with ionizing radiation, and the BRCA1 protein was visualized by immunofluorescence at varying times (Fig. 4A). Both cell types showed a clear response as indicated by a dramatic increase in the number of BRCA1-containing nuclear foci. However, as with other

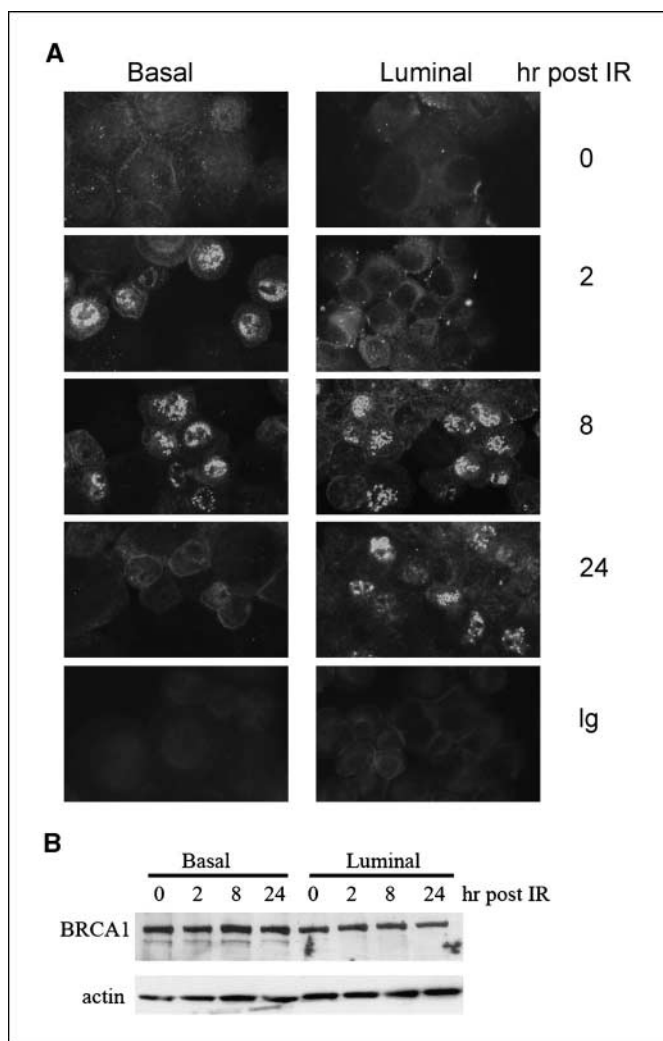


Figure 4. Kinetics of nuclear accumulation of BRCA1 protein after ionizing radiation in basal and luminal breast epithelial cells. *A*, cells were grown in monolayer culture, treated with 5 Gy of ionizing radiation, then harvested at the indicated time points and prepared for immunofluorescent detection using the monoclonal antibody, MS110. BRCA1 protein localized to intense nuclear foci in both cell types and in a large fraction of the cells during the course of the experiment. *B*, detection of total cellular BRCA1 protein by immunoblotting in basal and luminal cells treated with 5 Gy of ionizing radiation. Levels and mobility of the 220 kDa BRCA1 protein did not vary significantly over the course of the experiment or between the cell types.

measures of response studied, these foci seemed to dissipate by 24 h in the basal cells but persisted in the matched luminal population. Total BRCA1 protein as measured by immunoblotting was not significantly different between the two cell types or in response to ionizing radiation (Fig. 4B). BRCA1 nuclear focus formation is consistent with other measures of the DNA damage response in these cell types, further indicating that basal cells tend to have a much more transitory response than luminal cells. The underlying reason for this difference is not yet known.

Response to ionizing radiation in organ culture. There is one important caveat in the preceding experiments. The two cell types, although isogenic, derived at the same time, and cultured in parallel, were grown in different media (DFCI versus BCM). There is no direct way to control for this difference; therefore, our results could be interpreted as secondary to the culture conditions. To address this issue as directly as possible, we explored the use of primary organ cultures of human mammary tissue to measure the response to DNA damage. Not only would this approach control for culture conditions, it would also provide the three-dimensional structure and mesenchymal cells present in the natural setting. We obtained a fresh breast reduction specimen from a 34-year-old woman with no history of breast cancer, trimmed away the adipose tissue, and then cut the parenchyma into $\sim 3\text{-mm}^3$ fragments. These fragments were incubated overnight in a tissue culture dish containing DFCI and then were treated (or mock treated) with 5 Gy of ionizing radiation the next day. These fragments were harvested at varying time points after ionizing radiation and immediately embedded and frozen in matrix for histologic sectioning. Thin sections were prepared and analyzed by immunohistochemistry (Fig. 5). The fragments retained architecture (Fig. 5, *H&E*) typical of the normal mammary gland and through 24 h after ionizing radiation did not harbor apoptotic cells as measured by the absence of M30 antibody staining (detecting the caspase cleavage product of CK18; not shown). Nonirradiated fragments showed weak and relatively uniform p53 immunostaining. Two hours after ionizing radiation, we could detect the characteristic intense p53 nuclear staining indicative of activated p53 protein, but only in epithelia located in the basal layer. No cells in the luminal layer showed this type of accumulation. However, 24 h after ionizing radiation, we were able to detect numerous ductal structures that showed widespread nuclear staining for p53. No further accumulation in the basal layer was evident and, indeed, we could not identify any cells in the basal layer with staining comparable with that observed 2 h after ionizing radiation. Finally, phosphorylation of histone H2AX was also examined using an antibody specific for the activated form of this protein (41). We observed a dramatic increase in staining for this proximal marker of the DNA damage response over the course of 24 h. However, basal cells again showed a much more rapid reduction in the levels of phosphorylated H2AX than adjacent luminal cells. By 24 h after ionizing radiation, pH2AX staining is primarily in the luminal cells shown by the complementary staining with the basal cell marker, CALLA, in a parallel section. These results further support our finding that cells of basal origin have a rapid but transient response to a physical DNA-damaging agent, whereas luminal cells have a more prolonged response to the same genotoxic insult.

Discussion

The studies described here were prompted by a number of observations regarding breast cancer and *BRCA1*. As with any

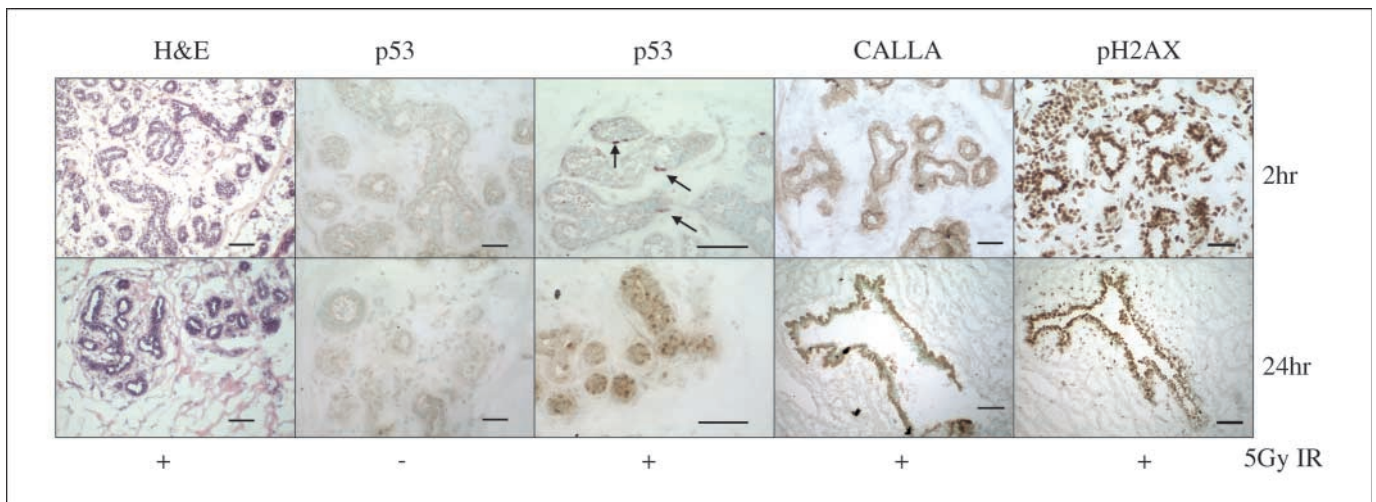


Figure 5. Response of normal *ex vivo* human mammary tissue to ionizing radiation. Fragments from a reduction mammoplasty were cultured in DFCI overnight before treatment with 5 Gy of ionizing radiation. Multiple fragments at each time point were harvested and embedded in matrix before sectioning. Thin sections were reacted with antibodies to p53, CALLA, and phosphorylated H2AX. H&E-stained sections are shown at 2 and 24 h after ionizing radiation. There is little nuclear accumulation of p53 protein without ionizing radiation treatment. *Arrows*, basal cells with characteristic nuclear accumulation of p53 protein at 2 h. By 24 h, detectable p53 protein is present primarily in the luminal compartment. CALLA reactivity shows the location of basal cells at 2 and 24 h after ionizing radiation. Staining with phosphorylated H2AX antibody shows intense reactivity in both layers at 2 h after ionizing radiation, whereas at 24 h, reactivity is largely diminished in the basal layer. Full size images are available at <http://data.cgt.duke.edu/Basalluminalradiation.php>. Bar, 50 μ m.

disease, a dissection of molecular etiology should be based on comparisons with the normal or baseline condition. For breast epithelium, the likely cell type of origin for breast cancer, many model systems have proven valuable in studying the normal biology. These models include animals (most often rodents but many mammals have been examined), normal mammary epithelial cells (human and otherwise) typically derived from breast reductions, and cell lines derived from normal mammary cells (immortalized by a number of different methods). Much of what we do know about human breast epithelium comes from work done on either short-term cultures of normal cells (HMEC) or immortalized derivatives thereof. The one common problem with these cells is that they have the characteristics of basal epithelium; therefore, most comparisons to cancer that have been made using these cell culture models removes the luminal cell from the equation. The exclusion of luminal cells has not been intentional; rather it is due to the fact that basal cells proliferate much better on plastic under the conditions that have been developed to culture breast epithelia.

The Ber-EP4 antibody recognizes the cell surface protein encoded by the *TACSTD1* gene, previously known by other names, notably *EpCAM* and *TROP1* (42). This antigen and antibodies recognizing it have primarily been used for detecting, purging, and treating occult carcinoma cells (24, 43). There is little information on the function of the *TACSTD1* protein outside of its role in cell adhesion (44). The significance of its bimodal expression pattern in basal versus luminal cells is unknown. Expression array data on 18 breast cancer cell lines indicated that MDA435, MDA231, BT549, HS578T, MDA157, and BT549 all expressed low levels of the *TACSTD1* message compared with the other lines in the study (Fig. 1B). All of these cell lines are *ESR1*, *PGR*, and *ERBB2* low or negative, indicative of the basal phenotype, lending further support that *TACSTD1* is expressed at much lower levels on cells in the basal lineage, both normal and neoplastic.

From the standpoint of cell purification, using a single antibody is significantly simpler than previous approaches. Cell purity, as assessed by morphology and expression profile, seemed to be very

good. Comparing lists of genes that were most differentially expressed in two other studies of basal and luminal mammary epithelial cells, we found excellent concordance even with the complication of different purification techniques and expression platforms (33, 34). Further, we analyzed gene expression after culturing the two cell types in selective medium, whereas the previous studies extracted RNA without prior culturing of the cells. Therefore, it seems that the purification and culture conditions allow the cells to retain their strong characteristic signatures.

Consistent with the work of Pechoux et al. (15), we also found that luminal cells could be readily trans-differentiated into basal-like cells simply by switching the medium but not vice versa. When basal cells are placed into medium containing high serum (luminal cell conditions), they cease proliferating, enlarge, and senesce. A natural conclusion from these properties is that the luminal cell population harbors cells that can be reprogrammed (i.e., stem cells). To further investigate this possibility, we measured the percentage of side population cells in the basal and luminal fractions. From three different early passage HMEC cultures, we found an equal number of dye excluding side population cells (~1%) in the two fractions, suggesting that stem like cells may have both luminal and basal characteristics.

Our primary purpose for culturing these cells was to investigate the nature of the DNA damage response. There is a wealth of evidence to support the following contentions. (a) The human breast exposed to ionizing radiation is prone to developing cancer. (b) Germ line mutations in the *BRCA1* gene predispose primarily to breast and ovarian cancer. (c) Breast cancers arising in women with *BRCA1* mutations are much more likely to have medullary histology and gene expression patterns consistent with basal-like tumors. (d) *BRCA1* is intimately involved in the response to DNA damage. (e) *BRCA1*, although associated with a highly specific set of cancers, does not have tissue-limited expression, a condition that is analogous to other germ line cancer susceptibility genes such as *RB* and *APC*. These findings prompted us to develop a system by which we could study tissue-specific effects of *BRCA1*

related to its etiologic role in breast cancer. The type of breast cancers that arise in women harboring mutations in *BRCA1* suggested that isogenic normal basal and luminal cells might be the most appropriate system to examine these effects. Further, because ionizing radiation and DNA damage resulting from it are linked not only to breast cancer but also to the mechanistic actions of *BRCA1*, it seemed logical to use this physical agent to analyze cellular response. Our findings in this regard are consistent and support the hypothesis that normal basal and luminal cells respond in a distinct manner to ionizing radiation.

Our results indicate that basal cells undergo a transitory cell cycle arrest after irradiation, whereas luminal cells have a more prolonged arrest, primarily at G₂-M. The behavior of molecular markers, including the kinetics of p53, p21, and *GADD45a* expression and *BRCA1* nuclear focus formation, are consistent with this picture. In addition, baseline expression of key cell cycle genes is significantly different in the two cell types. In particular, p53 protein, 14-3-3 σ , and p63 are all elevated in basal cells compared with luminal cells. From expression array data, both 14-3-3 σ and p63 are regulated at the RNA level, whereas p53 mRNA is in fact slightly more abundant in luminal cells. The p53 protein is most significantly regulated by changes in protein stability. Mutated versions of p53 accumulate in cells due to prolonged half-life; however, the stability of the wild-type protein is also highly variable in different normal cell types. In cycling fibroblasts and mammary epithelial cells, p53 protein half-life has been measured at 30 min and 4 h, respectively (45). As with most other experiments using HMEC, a predominantly basal cell population was used in the experiment measuring protein half-life. Therefore, we consider it likely that p53 protein stability is lower in breast luminal cells resulting in reduced steady-state levels compared with basal cells. Numerous factors and conditions are known to influence p53 stability; however, the mdm2 protein is still considered to be the central player (for review, see ref. 46). At least at the level of mRNA, *MDM2* is expressed at equivalent (and very low) levels in both basal and luminal cells.

Many factors could account for the differential response to ionizing radiation. It is conceivable that the amount of physical damage (i.e., strand breakage) is different in the two cell types, perhaps influenced by varying levels of free radicals after dosing. A number of enzymes participate in ameliorating oxidative damage, including the superoxide dismutases, catalases, glutathione peroxidases, and glutathione transferases. From array data, the most significant differences in the expression of these genes at the mRNA level are *SOD1* (approximately twice higher in luminal cells) and *GSTP1* (approximately thrice higher in basal cells). Either or both of these genes could modulate the amount of oxidative damage on DNA. A polymorphic variant in *GSTP1* has been examined in relation to oxidative damage with conflicting results (47, 48). On the other hand, SOD levels have been shown to directly correlate with reactive oxygen species and damage produced by free radicals (49). *SOD1*, at the RNA level, is more highly expressed in the luminal cells, suggesting that persistence of free radicals is not a primary cause of the observed transitory damage response in the basal cells. Another possibility is that DNA lesions are repaired more rapidly in basal cells, resulting in a less prolonged damage response. Our attempts to measure this directly using the comet assay were unsuccessful.

The purified and cultured basal and luminal cells could be useful for many studies of these lineages. For certain kinds of investigation, different culture conditions may not be important; however, we were specifically interested in a comparative study between the two

cell types. Of significant concern then were systematic biases that could be introduced from the respective tailored growth milieu. That the cell types retained expression patterns characteristic of uncultured basal and luminal cells mitigated this concern somewhat. In seeking to further address this issue, we explored the use of short-term primary organ cultures of normal human breast. Organ culture is perhaps the simplest possible system for studying the normal human breast *in vitro* and has been used to measure variables such as proliferation as a function of age, topography, and cell type (50). Although this type of system is not particularly amenable to genetic manipulation, it is well suited for the study of response to penetrating physical agents such as ionizing radiation. Analogous to the isolated cell populations, we observed a distinct response to ionizing radiation in the basal versus luminal layers. As would be anticipated, these responses are not uniform throughout each specimen. However, we discovered clear trends. Basal cells accumulated p53 protein very early after irradiation, whereas luminal cells had a delayed but more prolonged response. We have maintained similar organ cultures out to 17 days after explanting with maintenance of ductal organization and ongoing proliferation of the epithelia as measured by Ki-67 staining. This model may be extremely useful for studying both short-term and relatively long-term effects of physical and chemical agents on the breast epithelium *in situ*.

The basic hypothesis underlying these studies was that cells of the basal and luminal lineage exhibit a differential DNA damage response that could begin to explain the series of observations regarding breast cancer and *BRCA1* listed above. What we have shown is that by a number of different criteria, this is indeed the case. Given this differential response, a straightforward model can be constructed to account for the finding that *BRCA1* mutations result in tumors with a basal phenotype. Genotoxic events, whether extrinsic or intrinsic, act on ductal epithelial cells at a finite frequency. *BRCA1* and other molecular components of the damage response pathway are activated and serve to arrest cells, initiate a process of repair, or trigger apoptosis. In the luminal compartment, this is a robust and efficient cascade. Damage in basal cells does trigger these pathways; however, the response is much weaker. Therefore, these cells are more likely to escape arrest and/or apoptosis and accumulate genetic abnormalities; that is, they are more susceptible to neoplastic initiation and progression after DNA damage. Loss of *BRCA1*, first in a heterozygous and eventually in a homozygous state, serves to increase the severity of the situation by further blunting one of the key damage response pathways.

This theory is based on the possibility that different types of breast cancer arise from different precursor cells. The primary alternative concept is that all (or most) breast cancers are derived from a single cell type, the incompletely identified mammary stem cell. The heterogeneity of breast cancers then occurs through variations in the type of incident genetic and epigenetic events. Overexpression of the estrogen receptor (by as yet unidentified mechanisms) leads to one type of cancer, amplification of *ERBB2* leads to another, and so on, with combinations of the most common events giving rise to the observed spectrum of human breast cancer. These two concepts are not mutually exclusive. For example, the stem cell must give rise to fully differentiated basal and luminal cells. These terminally differentiated cells probably have limited proliferative capacity. Therefore, it is reasonable to assume that there are cells with intermediate phenotypes (i.e., committed precursor cells that continue to divide but are destined to give rise to basal or luminal cells). In fact, the majority of cells

grown as HMEC could be considered as having these properties. Although our data do not directly address these alternate possibilities, the clear finding of a differential response to DNA damage by normal basal versus luminal cells increases the likelihood that different cell populations may be naturally more or less sensitive to the actions of both carcinogenic agents and genetic events, both inborn and acquired.

Acknowledgments

Received 11/2/2006; revised 1/16/2007; accepted 1/25/2007.

Grant support: NIH grant CA84955 (J.R. Marks).

The costs of publication of this article were defrayed in part by the payment of page charges. This article must therefore be hereby marked *advertisement* in accordance with 18 U.S.C. Section 1734 solely to indicate this fact.

We thank Nancy Glover for her excellent technical assistance, and John Olson, Craig Bennett, and James Koh for their experimental and editorial input.

References

1. Sorlie T, Perou CM, Tibshirani R, et al. Gene expression patterns of breast carcinomas distinguish tumor subclasses with clinical implications. *Proc Natl Acad Sci U S A* 2001;98:10869–74.
2. Taylor-Papadimitriou J, Stampfer M, Bartek J, et al. Keratin expression in human mammary epithelial cells cultured from normal and malignant tissue: relation to *in vivo* phenotypes and influence of medium. *J Cell Sci* 1989;94:403–13.
3. Cattoretti G, Andreola S, Clemente C, D'Amato L, Rilke F. Vimentin and p53 expression on epidermal growth factor receptor-positive, oestrogen receptor-negative breast carcinomas. *Br J Cancer* 1988;57:353–7.
4. Tot T. The cytokeratin profile of medullary carcinoma of the breast. *Histopathology* 2000;37:175–81.
5. Orlando L, Renne G, Rocca A, et al. Are all high-grade breast cancers with no steroid receptor hormone expression alike? The special case of the medullary phenotype. *Ann Oncol* 2005;16:1094–9.
6. Pedersen L, Zedler K, Holck S, Schiodt T, Mouridsen HT. Medullary carcinoma of the breast. Prevalence and prognostic importance of classical risk factors in breast cancer. *Eur J Cancer* 1995;31A:2289–95.
7. Marcus JN, Watson P, Page DL, et al. Hereditary breast cancer—pathobiology, prognosis, and BRCA1 and BRCA2 gene linkage. *Cancer* 1996;77:697–709.
8. Lakhani SR, Easton DF, Stratton MR, et al. Pathology of familial breast cancer—differences between breast cancers in carriers of BRCA1 or BRCA1 mutations and sporadic cases. *Lancet* 1997;349:1505–10.
9. Foulkes WD, Stefansson IM, Chappuis PO, et al. Germline BRCA1 mutations and a basal epithelial phenotype in breast cancer. *J Natl Cancer Inst* 2003;95:1482–5.
10. Hedenfalk I, Duggan D, Chen Y, et al. Gene-expression profiles in hereditary breast cancer. *N Engl J Med* 2001;344:539–48.
11. Esteller M, Silva JM, Dominguez G, et al. Promoter hypermethylation and BRCA1 inactivation in sporadic breast and ovarian tumors. *J Natl Cancer Inst* 2000;92:564–9.
12. Osin P, Lu YJ, Stone J, et al. Distinct genetic and epigenetic changes in medullary breast cancer. *Int J Surg Pathol* 2003;11:153–8.
13. Petersen OW, van Deurs B. Growth factor control of myoepithelial-cell differentiation in cultures of human mammary gland. *Differentiation* 1988;39:197–215.
14. Petersen OW, Van DB. Preservation of defined phenotypic traits in short-term cultured human breast carcinoma derived epithelial cells. *Cancer Res* 1987;47:856–66.
15. Pechoux C, Gudjonsson T, Ronnov-Jessen L, Bissell MJ, Petersen OW. Human mammary luminal epithelial cells contain progenitors to myoepithelial cells. *Dev Biol* 1999;206:88–99.
16. Hammond SL, Ham RG, Stampfer MR. Serum-free growth of human mammary epithelial cells: rapid clonal growth in defined medium and extended serial passage with pituitary extract. *Proc Natl Acad Sci U S A* 1984;81:5435–9.
17. Band V, Sager R. Distinctive traits of normal and tumor derived human mammary epithelial cells expressed in a medium that supports long term growth of both cell types. *Proc Natl Acad Sci U S A* 1989;86:1249–53.
18. Gomm JJ, Browne PJ, Coope RC, Liu QY, Buluwela L, Coombes RC. Isolation of pure populations of epithelial and myoepithelial cells from the normal human mammary gland using immunomagnetic separation with Dynabeads. *Anal Biochem* 1995;226:91–9.
19. Dontu G, Abdallah WM, Foley JM, et al. *In vitro* propagation and transcriptional profiling of human mammary stem/progenitor cells. *Genes Dev* 2003;17:1253–70.
20. Marks JR, Lin J, Hinds P, Miller D, Levine AJ. Cellular gene expression in papillomas of the choroid plexus from transgenic mice that express the simian virus 40 large T antigen. *J Virol* 1989;63:790–7.
21. Vaughn JP, Davis PL, Jarboe MD, et al. BRCA1 expression is induced prior to DNA synthesis in both normal and tumor derived breast cells. *Cell Growth Differ* 1996;7:711–5.
22. Latza U, Niedobitek G, Schwarting R, Nekarda H, Stein H. Ber-EP4: new monoclonal antibody which distinguishes epithelia from mesothelial. *J Clin Pathol* 1990;43:213–9.
23. Bild AH, Yao G, Chang JT, et al. Oncogenic pathway signatures in human cancers as a guide to targeted therapies. *Nature* 2006;439:353–7.
24. Rao CG, Chianese D, Doyle GV, et al. Expression of epithelial cell adhesion molecule in carcinoma cells present in blood and primary and metastatic tumors. *Int J Oncol* 2005;27:49–57.
25. Band V, Zajchowski D, Kulesa V, Sager R. Human papilloma virus DNAs immortalize normal human mammary epithelial cells and reduce their growth factor requirements. *Proc Natl Acad Sci U S A* 1990;87:463–7.
26. Tibshirani R, Hastie T, Narasimhan B, Chu G. Diagnosis of multiple cancer types by shrunken centroids of gene expression. *Proc Natl Acad Sci U S A* 2002;99:6567–72.
27. Barbareschi M, Pecciarini L, Cangi MG, et al. p63, a p53 homologue, is a selective nuclear marker of myoepithelial cells of the human breast. *Am J Surg Pathol* 2001;25:1054–60.
28. Egan MJ, Newman J, Crocker J, Collard M. Immunohistochemical localization of S100 protein in benign and malignant conditions of the breast. *Arch Pathol Lab Med* 1987;111:28–31.
29. Phillips K, Park MA, Quarrie LH, et al. Hormonal control of IGF-binding protein (IGFBP)-5 and IGFBP-2 secretion during differentiation of the HC11 mouse mammary epithelial cell line. *J Mol Endocrinol* 2003;31:197–208.
30. Petraki CD, Karavana VN, Skoufogiannis PT, et al. The spectrum of human kallikrein 6 (zyme/protease M/neurosin) expression in human tissues as assessed by immunohistochemistry. *J Histochem Cytochem* 2001;49:1431–41.
31. Galgano MT, Hampton GM, Frierson HF. Comprehensive analysis of HE4 expression in normal and malignant human tissues. *Mod Pathol* 2006;19:847–53.
32. Reis FM, Luisi S, Carneiro MM, et al. Activin, inhibin and the human breast. *Mol Cell Endocrinol* 2004;225:77–82.
33. Jones C, Mackay A, Grigoriadis A, et al. Expression profiling of purified normal human luminal and myoepithelial breast cells: identification of novel prognostic markers for breast cancer. *Cancer Res* 2004;64:3037–45.
34. Allinen M, Beroukhim R, Cai L, et al. Molecular characterization of the tumor microenvironment in breast cancer. *Cancer Cell* 2004;6:17–32.
35. Bunting KD. ABC transporters as phenotypic markers and functional regulators of stem cells. *Stem Cells* 2002;20:11–20.
36. Stefanou D, Batistatou A, Nonni A, Arkoumani E, Agnantis NJ. p63 expression in benign and malignant breast lesions. *Histol Histopathol* 2004;19:465–71.
37. Komarova EA, Zelnick CR, Chin D, et al. Intracellular localization of p53 tumor suppressor protein in γ -irradiated cells is cell cycle regulated and determined by the nucleus. *Cancer Res* 1997;57:5217–20.
38. Ferguson AT, Evron E, Umbricht CB, et al. High frequency of hypermethylation at the 14–3-3 σ locus leads to gene silencing in breast cancer. *Proc Natl Acad Sci U S A* 2000;97:6049–54.
39. Scully R, Chen JJ, Ochs RL, et al. Dynamic changes of BRCA1 subnuclear location and phosphorylation state are initiated by DNA damage. *Cell* 1997;90:425–35.
40. Greenberg RA, Sobhian B, Pathania S, Cantor SB, Nakatani Y, Livingston DM. Multifactorial contributions to an acute DNA damage response by BRCA1/BARD1-containing complexes. *Genes Dev* 2006;20:34–46.
41. Paull TT, Rogakou EP, Yamazaki V, Kirchgessner CU, Gellert M, Bonner WM. A critical role for histone H2AX in recruitment of repair factors to nuclear foci after DNA damage. *Curr Biol* 2000;10:886–95.
42. Calabrese G, Crescenzi C, Morizio E, Palka G, Guerra E, Alberti S. Assignment of TACSTD1 (alias TROP1, M4S1) to human chromosome 2p21 and refinement of mapping of TACSTD2 (alias TROP2, M1S1) to human chromosome 1p32 by *in situ* hybridization. *Cytogenet Cell Genet* 2001;92:164–5.
43. Went P, Vasei M, Bubendorf L, et al. Frequent high-level expression of the immunotherapeutic target EpCAM in colon, stomach, prostate and lung cancers. *Br J Cancer* 2006;94:128–35.
44. Ladwein M, Pape UF, Schmidt DS, et al. The cell-cell adhesion molecule EpCAM interacts directly with the tight junction protein claudin-7. *Exp Cell Res* 2005;309:345–57.
45. Delmolino L, Band H, Band V. Expression and stability of p53 protein in normal human mammary epithelial cells. *Carcinogenesis* 1993;14:827–32.
46. Lavin MF, Gueven N. The complexity of p53 stabilization and activation. *Cell Death Differ* 2006;13:941–50.
47. Hernandez A, Xamena N, Gutierrez S, et al. Basal and induced micronucleus frequencies in human lymphocytes with different GST and NAT2 genetic backgrounds. *Mutat Res* 2006;606:12–20.
48. Matsui A, Ikeda T, Enomoto K, et al. Increased formation of oxidative DNA damage, 8-hydroxy-2'-deoxyguanosine, in human breast cancer tissue and its relationship to GSTP1 and COMT genotypes. *Cancer Lett* 2000;151:87–95.
49. Davis CA, Hearn AS, Fletcher B, et al. Potent anti-tumor effects of an active site mutant of human manganese-superoxide dismutase. Evolutionary conservation of product inhibition. *J Biol Chem* 2004;279:12769–76.
50. Russo J, Calaf G, Roi L, Russo IH. Influence of age and gland topography on cell kinetics of normal human breast tissue. *J Natl Cancer Inst* 1987;78:413–8.

Cancer Research

The Journal of Cancer Research (1916–1930) | The American Journal of Cancer (1931–1940)

Isogenic Normal Basal and Luminal Mammary Epithelial Isolated by a Novel Method Show a Differential Response to Ionizing Radiation

Gudrun Huper and Jeffrey R. Marks

Cancer Res 2007;67:2990-3001.

| | |
|-------------------------------|---|
| Updated version | Access the most recent version of this article at: http://cancerres.aacrjournals.org/content/67/7/2990 |
| Supplementary Material | Access the most recent supplemental material at: http://cancerres.aacrjournals.org/content/suppl/2007/03/30/67.7.2990.DC2 |

| | |
|------------------------|--|
| Cited articles | This article cites 50 articles, 21 of which you can access for free at: http://cancerres.aacrjournals.org/content/67/7/2990.full.html#ref-list-1 |
| Citing articles | This article has been cited by 5 HighWire-hosted articles. Access the articles at: /content/67/7/2990.full.html#related-urls |

| | |
|-----------------------------------|---|
| E-mail alerts | Sign up to receive free email-alerts related to this article or journal. |
| Reprints and Subscriptions | To order reprints of this article or to subscribe to the journal, contact the AACR Publications Department at pubs@aacr.org . |
| Permissions | To request permission to re-use all or part of this article, contact the AACR Publications Department at permissions@aacr.org . |